HHS Public Access

Author manuscript

Anal Chem. Author manuscript; available in PMC 2017 February 10.

Published in final edited form as:

Anal Chem. 2016 January 19; 88(2): 1336–1344. doi:10.1021/acs.analchem.5b03794.

Analysis of Antiretrovirals in Single Hair Strands for Evaluation of Drug Adherence with Infrared-Matrix-Assisted Laser Desorption Electrospray Ionization Mass Spectrometry Imaging

Elias P. Rosen[†,*], **Corbin G. Thompson**[†], **Mark T. Bokhart**[‡], **Heather M. A. Prince**[§,‖], **Craig Sykes**[†,‖], **David C. Muddiman**[‡], and **Angela D. M. Kashuba**[†,§,‖]

[†]Eshelman School of Pharmacy, University of North Carolina, Chapel Hill, North Carolina 27599, United States

[‡]W.M. Keck FTMS Laboratory for Human Health Research, Department of Chemistry, North Carolina State University, Raleigh, North Carolina 27695, United States

[§]School of Medicine, University of North Carolina, Chapel Hill, North Carolina 27599, United States

[‖]Center for AIDS Research, University of North Carolina, Chapel Hill, North Carolina 27599, United States

Abstract

Adherence to a drug regimen can be a strong predictor of health outcomes, and validated measures of adherence are necessary at all stages of therapy from drug development to prescription. Many of the existing metrics of drug adherence (e.g., self-report, pill counts, blood monitoring) have limitations, and analysis of hair strands has recently emerged as an objective alternative. Traditional methods of hair analysis based on LC–MS/MS (segmenting strands at ≥1 cm length) are not capable of preserving a temporal record of drug intake at higher resolution than approximately 1 month. Here, we evaluated the detectability of HIV antiretrovirals (ARVs) in hair from a range of drug classes using infrared matrix-assisted laser desorption electrospray ionization (IR-MALDESI) mass spectrometry imaging (MSI) with 100 μm resolution. Infrared laser desorption of hair strands was shown to penetrate into the strand cortex, allowing direct measurement by MSI without analyte extraction. Using optimized desorption conditions, a linear correlation between IR-MALDESI ion abundance and LC–MS/MS response was observed for six common ARVs with estimated limits of detection less than or equal to 1.6 ng/mg hair. The distribution of efavirenz (EFV) was then monitored in a series of hair strands collected from HIV infected, virologically suppressed patients. Because of the role hair melanin plays in accumulation

[*]**Corresponding Author**. Phone: 919-962-5151. eli@unc.edu.

ASSOCIATED CONTENT

Supporting Information

The Supporting Information is available free of charge on the ACS Publications website at DOI: 10.1021/acs.analchem.5b03794.

Summary of ARV physicochemical properties, evaluation of IR-MALDESI extraction efficiency, detailed summary of IR-MALDESI calibration with incubated and dosed hair, PTCA response to dosed hair, and summary of lipid-like endogenous ions in hair measured by IRMALDESI (PDF)

The authors declare no competing financial interest.

of basic drugs (like most ARVs), an MSI method to quantify the melanin biomarker pyrrole-2,3,5-tricarboxylic acid (PTCA) was evaluated as a means of normalizing drug response between patients to develop broadly applicable adherence criteria.

Graphical Abstract

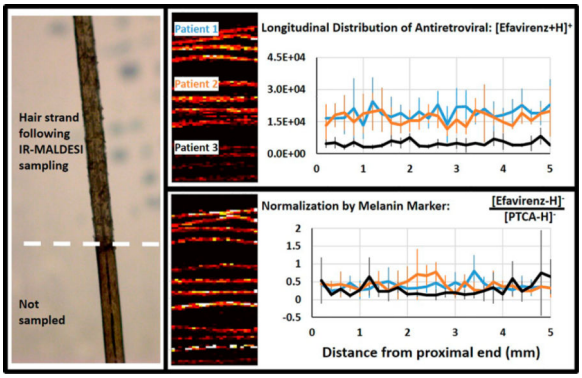

Adherence to antiretroviral (ARV) therapy is critical for achieving HIV RNA suppression in HIV-infected patients[1–3] and for preventing HIV acquisition in uninfected individuals using pre-exposure prophylaxis (PrEP).[4] Yet a high level of adherence is challenging for HIV-infected individuals on life-long ARVs and for HIV-negative individuals using daily PrEP who are not at daily risk for HIV acquisition. Poor adherence was primarily responsible for a lack of drug effectiveness in multiple recent double-blind, placebo-controlled PrEP studies.[5–7] These studies found that counting product returns and using patient self-report significantly overpredicted adherence as measured by ARV concentrations in blood plasma or cells. Since the consequences of poor or intermittent adherence are significant, valid measures of adherence are critical for optimizing the effectiveness of both HIV treatment and prevention, in both the clinic and research settings. Hair has long been a targeted analysis matrix for forensic monitoring of drug abuse[8,9] because its temporal record (weeks–months) provides a longer term for retrospective analysis than other human matrixes and is being increasingly utilized for therapeutic drug monitoring.[10,11]

Currently, the disposition of ARVs in hair is measured by LC–MS/MS analysis.[12,13] This approach represents the current “gold standard” and has been correlated with adherence in PrEP[14] and with health outcomes in treatment.[15,16] While LC–MS/MS methods are sensitive and specific, these techniques require multiple (e.g., 25–100) strands of at least 1 cm in length to be combined for a single measurement. This approach effectively averages drug response over a month’s time based on growth rates for hair in the active, anagen, phase of hair growth[9] and cannot differentiate strict adherence to therapy at regular dosing intervals from heterogeneous adherence. The admixture of various exposures within such a homogenate can lead to hybrid hair drug concentration which may over- or underestimate drug exposure at any one point in time. Given that periodic self-imposed cessation from treatment (“drug holidays”) for periods greater than 48 h can be associated with rebounding viral loads[17] and treatment failure due to development of drug resistance,[18] a smaller temporal window of adherence monitoring would be beneficial to inform evaluation of drug

efficacy and strategy for care. Additionally, LC–MS/MS methods have a potentially burdensome requirement for quantity of donated hair and necessitate a time intensive sample preparation.

Mass spectrometry imaging (MSI) of biological samples offers an alternative analytical approach providing the capability for simultaneously monitoring the spatial distribution of analytes ranging from small molecules, such as pharmaceutical drugs,[19] to lipids[20,21] to peptides and proteins.[22] The utility of MSI has been demonstrated for a variety of fields, with particular emphasis on biomedical applications like drug distribution[23] and biomarker identification.[24] While such studies predominately target biological tissue as a sample matrix, recent work has investigated the distribution of pharmaceuticals,[25] drugs of abuse,[26–29] and endogenous biomolecules[30] in hair using multiple MSI techniques.

In this work, we extend the application of infrared matrix-assisted laser desorption electrospray ionization (IR-MALDESI),[31] which we have demonstrated to be a sensitive MSI technique for the analysis of ARVs in biological tissue,[32–34] to the morphologically distinct matrix of hair. The technique couples resonant laser desorption with electrospray postionization for a soft, ESI-like ionization mechanism. Unlike MALDI, the traditional approach for MSI, IR-MALDESI does not require an organic matrix to promote analyte desorption and ionization, which can interfere with the analysis of small molecules such as ARVs. Instead, a layer of ice deposited on the sample is used as an energy-absorbing matrix for infrared radiation that is easily applied and does not contribute to the background MS response. An evaluation of variables controlling the desorption of material from a single hair strand was performed to maximize analyte response by IR-MALDESI. These conditions were then used to determine the IRMALDESI response to a broad range of ARVs representing several drug classes, which has been correlated to LC–MS/MS analyses for concentrations ranging 3 orders of magnitude. The distribution of ARVs within single hair strands collected from HIV+ patients on active ARV therapy is evaluated here for the first time.

Additionally, an MSI method for determining relative hair melanin content is demonstrated, providing a critical means of comparing drug exposure in hair strands collected from different patients. During the hair growth process, averaging 1 cm per month on the scalp, three factors predominately contribute to the incorporation of drug in hair strands: drug basicity, drug lipophilicity, and hair melanin content.[9] The former two physicochemical attributes of the drug control its ability to penetrate cellular membranes of hair, where the drug then binds to melanin. Hence, preferential accumulation has been observed for lipophilic and basic drugs in pigmented hair strands, with drug concentration correlating with melanin concentration[35–37] or otherwise present among race groups possessing higher melanin in hair.[38] Here, we examine a MSI hair sample preparation step to oxidize and chemically degrade polymeric melanin into smaller molecules used as direct markers of pigmentation.[39–41] We show that normalizing drug response in hair based on melanin content can facilitate comparison of drug response in hair between patients.

EXPERIMENTAL SECTION

Materials

Antiretroviral reference compounds emtricitabine (FTC), tenofovir (TFV), efavirenz (EFV), dolutegravir (DTG), raltegravir (RAL), darunavir (DRV), maraviroc (MRV), and lamivudine (3TC) were obtained through the NIH AIDS Reagent Program. Pyrrole-2,3,5-tricarboxylic acid (PTCA) acetic acid salt was purchased from Toronto Research Chemicals (Toronto, Ontario, CAN). Internal standard components FTC-$^{13}C^{15}N_2$ and TFV-$^{13}C_5$ were purchased from Moravek Biochemicals (CA), 3TC-^{15}N-d_2 and DRV-d_9 from Aptochem (Montreal, Canada), and RAL-d_3 and MVC-d_6, from Toronto Research Chemicals (Toronto, Canada). HPLC grade methanol and formic acid were purchased from Fisher Scientific (PA). Hydrogen peroxide (30%) was purchased from VWR International (PA). All materials were used without further purification.

Hair Samples

Sample collection occurred in accordance with Good Clinical Practice procedures, all applicable regulatory requirements, and the guiding principles of the Declaration of Helsinki. The study protocol was approved by the Biomedical Institutional Review Board at the University of North Carolina at Chapel Hill (IRBIS 08-0047), and all subjects provided written informed consent before study entry. Hair strands collected from a healthy donor not on HIV therapy were used both as negative controls and also as a blank hair matrix for incubation in a solution of ARVs. Blank hair was incubated in 1 mL of tissue culture media [Iscove's Modified Dulbecco's Media (Gibco, Grand Island, NY), 10% fetal bovine serum (Gibco), 240 units/mL nystatin (Sigma, St. Louis, MO), 100 units/mL penicillin-streptomycin (Gibco), and MEM vitamin solution (Sigma)] containing 6 ARVs (EFV, DTG, RAL, DRV, MRV, 3TC) ranging in concentration over 3 logs (1, 10, 100 μg/mL) for 24 h at 37 °C, allowing penetration of drug into the hair matrix, before the incubated strands were rinsed surficially with methanol/water and dried. ARV-incubated hair strands were used to optimize IR-MALDESI desorption conditions and calibrate instrument response to ARVs in hair. Hair strands were also collected at the UNC Clinical and Translational Research Center from HIV+, virologically suppressed subjects (<50 copies/ml RNA by PCR) receiving Atripla (a fixed dose combination of EFV, FTC, and prodrug form of TFV) for ≥1 year. Hair was collected from the occipital region of the scalp by lifting the top layer of hair and clipping 20–30 fibers of hair at least 1 cm long from as close to the scalp as possible. All hair samples were stored in aluminum foil and sealed in a plastic bag with desiccant until analysis.

Sample Preparation

Hair samples were adhered to glass microscope slides using double-sided adhesive tape without any prewashing. No solvent extraction step or sample manipulation was undertaken prior to MSI analysis when targeting disposition of ARVs in hair. For analysis of PTCA as a marker of eumelanin content in hair, sample-mounted slides were sprayed with a solution of 15% hydrogen peroxide and 1 M NH_4OH in 50/50 (v/v) methanol/water using a thermal-assisted pneumatic sprayer (TM Sprayer, LEAP Technologies) and allowed to incubate on a lab bench at room temperature for 24 h prior to analysis.

IR-MALDESI Mass Spectrometry Imaging

The components and working principles of the IR-MALDESI MSI source used in this work have been detailed elsewhere,[42] based on the original source design[31] and will be described here briefly. Sample slides for analysis were placed onto a Peltier-cooled sample stage where a controlled layer of ice was allowed to deposit onto the sample surface, which has been shown to enhance observed IR-MALDESI ion abundances.[43] The ice layer thickness was maintained throughout analysis by holding the relative humidity in the source enclosure at 10% using a low flow of dry nitrogen gas. A 100 Hz IR Opolette HR infrared OPO laser (Opotek, Carlsbad, CA) tuned to the asymmetric stretching vibrational mode of liquid water (λ = 2.94 μm) was used to desorb sample material. The plume of neutral material generated by laser desorption of the sample expanded upward from the stage and was ionized with an orthogonal electrospray plume in an ESI-like fashion.[44,45] Positive polarity experiments were conducted using a 50/50 (v/v) solution of methanol/water with 0.2% formic acid as the electrospray solvent. For polarity switching experiments, a 20 mM ammonium hydroxide modifier was used with the 50/50 (v/v) solution of methanol/water, as has been used previously.[46] A recent evaluation of solvent modifiers for polarity switching experiments, conducted after the work presented here was performed, indicates that increased ion abundance is gained when using an acetic acid modifier without bias of response between positive and negative ionization modes[47] and will be utilized in future work. Spatial resolution of 100 μm was achieved from the ~250 μm diameter laser spot by translating the two-axis stage in 100 μm increments based on an oversampling approach.[48] Resulting voxel dimensions for positive polarity experiments (100 μm × 100 μm) represent a theoretical temporal window of approximately 7 h based on an average growth rate of 1 cm per month. The method of data acquisition for polarity switching elongates the voxel dimension along one axis (200 μm × 100 μm) since the measurement polarity is alternated between sampling points across a scanline. The IR-MALDESI imaging source was fully synchronized with a Thermo Fisher Scientific Q Exactive Plus mass spectrometer (Bremen, Germany). The Q Exactive Plus was operated in full scan mode with a mass range *m/z* 150–600, with mass resolving power set to 140 000 (fwhm, *m/z* 200). Since AGC is turned off during IR-MALDESI experiments, lock masses are utilized in the control software to achieve parts per million mass accuracy.[49] For positive ionization mode two peaks of an ambient ion, diisooctyl phthalate, at *m/z* 391.2843 $[M + H]^+$ and *m/z* 413.2662 $[M + Na]^+$ were used as lock masses. The peaks of palmitic acid at *m/z* 255.2329 $[M - H]^-$ and stearic acid at *m/z* 283.2643 $[M - H]^-$ were used as lock masses in negative ionization mode. MS^2 imaging (MS^2I) of PTCA ($[M - H]^-$ *m/z* 198.0039) was conducted with a 0.5 *m/z* window centered at *m/z* 198.00 followed by ion accumulation in the C-trap. The accumulated ion packet was fragmented in the HCD cell at a normalized collision energy of 10% and then analyzed with mass resolving power of 140 000 (fwhm, *m/z* 200). All Thermo RAW files were converted first to mzML[50] and then imzML[51] file formats before data processing and analysis of MSI data using MSiReader.[52] Ion maps were created with a mass tolerance of 5 ppm, and sample dimensions are indicated by scale bars.

LC–MS/MS Analysis of Hair

Extraction of analytes from snippets (1–2 cm) of incubated hair strands and from intact (3–3.5 cm) dosed hair strands was performed at room temperature by 10 min of sonication and

20 min of vortexing in 0.300 mL of 70:30 methanol/water. Following extraction, the samples were mixed with isotopically labeled internal standards (FTC-$^{13}C^{15}N_2$, 3TC-^{15}N-d_2, TFV-$^{13}C_5$, RAL-d_3 (for RAL and DTG quantitation), MVC-d_6, and DRV-d_9 (for DRV and EFV quantitation)). Sample extracts were then evaporated to dryness and reconstituted in 90:10 water/methanol. A Shimadzu HPLC system performed chromatographic separation with a Waters Atlantis T3 (50 mm × 2.1 mm, 3 μm) analytical column under gradient conditions. An AB SCIEX API 5000 mass spectrometer (AB SCIEX, Foster City, CA) equipped with a turbo spray interface was used as the detector. The samples were analyzed with a set of calibration standards and QC samples prepared at 1 mg/mL in DMSO (DTG), methanol (DRV, EFV, MRV), and water (RAL, 3TC) and serially diluted in 70:30 methanol/water to cover an analytical range of 0.06–150 ng/sample. Extraction efficiency was evaluated based on analyte recovery from serial extraction of hair strands.[12] Precision and accuracy of the calibration standards and QC samples were within acceptance criteria of 20%.

RESULTS AND DISCUSSION

Optimization of IR-MALDESI for Hair Analysis

The analytical response of IR-MALDESI is sensitive to a range of variables in its experimental geometry controlling sample desorption and ionization, which have been previously optimized for interrogation of tissue cryosections.[53] Intact hair strands, roughly 80 μm in diameter and consisting of three distinct layers (cuticle, cortex, and medulla), present a distinct morphology relative to tissue cryosections. While incorporation of drug into hair can occur from the exterior cuticle layer through exposure to sweat and sebum, incorporation from blood occurs during follicular cell development and concentrates in the cortex.[9] MSI analysis of hair strands using UV lasers, with depth penetration on the order tens of nanometers,[54] typically includes preprocessing steps to facilitate probing analytes localized within the cortex either through solvent extraction[25] or by longitudinally sectioning[27] and abraiding[28] individual strands to expose the cortex directly. These methods add both labor and time to the analysis process, while also introducing the potential for sample contamination[28] and analyte delocalization[25] that may compromise the temporal record of drug use. Given the greater penetration depth (micrometers) of IR lasers into biological samples,[54] we sought to develop an IR-MALDESI analysis method for hair that did not require sample manipulation. We first investigated the extent to which the unique morphology of hair strands required different IR-MALDESI desorption conditions (sample height, laser fluence, and number of laser shots per voxel) than tissue to optimize response to ARVs. Hair strands incubated in EFV were used as a test matrix. Although the radial distribution of drug in hair may vary between incubated strands (where external drug solution is absorbed through the exterior of the strand) and physiologically incorporated strands, incubated strands have the advantage of representing a controlled reference sample in which drug is expected to be uniformly distributed for calibration of MSI response in quantitative hair analysis.[25] A representative optical image of a hair strand analyzed by IR-MALDESI can be seen in Figure 1A. The image shows a region of the strand that has not been analyzed, in which the pigmented, optically translucent strand with darker medulla layer is clearly visible. While profilometry measuring the laser penetration depth was not

performed, the change in opacity of the medulla and surrounding strand suggests that infrared laser desorption penetrates through the cuticle layer and potentially the cortex layer as well. Figure 1B shows ion maps of cholesterol ($[M + H - H_2O]^+$, *m/z* 369.3516) and EFV ($[M + H]^+$, *m/z* 316.0347) from IR-MALDESI analysis of incubated hair strands analyzed with varying numbers of laser shots (1–5) acquired at each volumetric element, or voxel, probed by the laser. Average ion abundances of EFV and endogenous lipids indicated that two laser shots per voxel, with a laser pulse of 0.6 mJ/pulse, yielded the best IR-MALDESI response to analytes in hair. Since the strand is not completely ablated with <5 laser pulses, the preference for two laser pulses may reflect the concentration of incorporated EFV closer to the surface of the strand or may also be a result of unfavorable effects on analyte ion abundance recently shown to occur as the C-trap accumulation time is extended to accommodate a greater number of laser pulses.[42] Reanalysis of a hair strand by IR-MALDESI, profiling a region in which the cuticle and some of the cortical layer had been previously removed by laser desorption, indicated a ~60% reduction in signal abundance of EFV (Figure S-1). This suggests that approximately 80%, as an upper bound, of accumulated EFV is extracted from incubated hair strands during initial IR-MALDESI analysis of intact hair.

Calibration of IR-MALDESI Response to ARVs in Incubated Hair and Correlation to LC–MS/MS

Using conditions yielding the best response to incubated strands, a calibration was performed of IR-MALDESI response to hair strands incubated in six ARVs: EFV, DTG, DRV, RAL, MRV, and 3TC. These ARVs, summarized in Table S-1, represent a range of drug classes often utilized in HIV treatment and which possess different basicity and lipophilicity controlling their incorporation into hair. Hair strands were incubated in a 3-log concentration range (1, 10, 100 μg/mL solutions) of the six ARVs as described above. Representative hair IR-MALDESI ion maps of ARV distribution in hair for EFV can be seen in Figure 2A for each of the three incubated drug concentrations. The averaged ion abundance of the ARVs from five individual strands measured by IR-MALDESI was compared to LC–MS/MS response, where the amount of drug in fixed segment lengths of individual strands is estimated based on hair mass using an average hair density (0.633 g/cm^3) and hair diameter (80 μm).[25] A complete summary of calibration data including linear plots of IR-MALDESI response to each of the six ARVs and blank samples can be found in the Supporting Information (Table S-2 and Figure S-2). These data are shown in Figure 2B, plotted on a log–log scale to allow IR-MALDESI response to all ARVs to be seen easily. Data are color-coded by available information on drug pK_a,[55–60] increasing in shade from 3TC (pK_a = 4.3)[60] to EFV (pK_a = 10.2).[56] Focusing on the cross-hatched data points, representing the lowest incubation concentration for each of the ARVs, it is observed that the amount of drug penetrating into hair strands as quantified by LC–MS/MS tends to increase with reported pK_a. The range of ARV concentrations in incubated strands scales in a similar manner, increasing from 3TC (1.00–61.76 ng/mg hair) to EFV (24.34–1772.58 ng/mg hair). LC–MS/MS extraction efficiencies for each ARV from incubated strands were estimated to be 86% or higher. A linear relationship (R^2 > 0.962) between IR-MALDESI response and LC–MS/MS exists over the entire range of concentrations for each ARV with the exception of DTG (R^2 = 0.645), as summarized in Table S-3. Intercept values for linear regressions

exceed IR-MALDESI response to blank samples, particularly for RAL, EFV, and DTG. Fits for these higher accumulating ARVs may be influenced by ion losses due to space charging[49] at the high end of the calibration range, where high IR-MALDESI ion abundance (>10^6) and variability are seen, at incubated hair concentrations greater than 300 ng/mg hair. Accumulation of ARVs in dosed hair is typically below 100–150 ng/mg hair,[14–16,61,62] and IR-MALDESI response to all six ARVs is highly linear (R^2 > 0.984) over this range (Figure S-2).[49]

IR-MALDESI signal abundance for a given analyte concentration varies according to the ionization efficiency of the analyte in the electrospray,[33] and the current MSI conditions indicate an increase in sensitivity from MRV > DTG > RAL > 3TC > DRV > EFV based on calibration slope. Limits of detection (LOD) were not reached experimentally for any of the six ARVs over the 3-log range in drug concentrations used for incubating hair strands but have been estimated to be less than or equal to 1.6 ng/mg hair based on the calibration and response to blank hair strands (Table S3). A systematic determination of instrumental LOD will be the focus of future work targeting ARV analysis in hair.

IR-MALDESI Response to ARVs in Dosed Hair

Brown hair strands cut from the scalp of three HIV infected, virologically suppressed subjects receiving fixed-dose Atripla (a combination of EFV, FTC, and prodrug form of TFV) for ≥1 year, were evaluated to determine interpatient and intrapatient variability in IR-MALDESI response. MSI analysis was simultaneously performed on 5–10 single hair strands from each HIV positive donor on ARV therapy to account for natural variability in hair growth cycles that can influence the accumulation of drug, with up to 20% of scalp hair in the dormant telogen phase as well as incubated strands used as positive controls. The resulting ion maps, Figure 3A, showed continuous distribution of EFV response across the entirety of each strand of hair without detectable gaps, indicating uninterrupted dosing in accordance with the condition of virologic suppression measured by PCR by which these patients were classified as adherent. MS^2I of dosed and incubated hair strands by IR-MALDESI confirmed the unique assignment of EFV based on known transition patterns.[63] The MSiSlicer feature of MSiReader allows visualization and interpretation of ion abundance along the curvilinear path of a hair strand. Figure 3B shows the temporal profile of EFV over 3 mm of a hair strand from Patient 1 starting at the proximal end, corresponding to approximately 9 days of hair growth. Pervoxel MSI response was evaluated using MSiReader software and average response for each patient is summarized in Figure 3A. Average IR-MALDESI response to multiple strands from individual donors indicated high repeatability (<12% relative standard deviation, % RSD) of response and a ~1.4-fold intrapatient variability in IR-MALDESI EFV ion abundance. A ~4-fold interpatient variability was observed. These results were in good agreement with LC–MS/MS analysis of extracts from matching single strands, Figure S-3, which indicated a ~2.3-fold interpatient variability in EFV (mean =1.720 ng/mg hair, range = 0.968–2.200 ng/mg hair). LC–MS/MS extraction efficiency for EFV from dosed hair was estimated to be 91% based on serial extraction of hair strands. No detectable response to TFV or FTC was observed by IR-MALDESI MSI from dosed patient samples. LC–MS/MS analysis of extracts from matching single strands indicated that FTC (mean = 0.333 ng/mg hair, range = 0.213–0.535

ng/mg hair) was present in the hair strands at concentrations below EFV and that TFV was below the limit of quantitation. TFV (pK_a = 3.75) and FTC (pK_a = 2.7) accumulate at low levels in hair and typically require large thatches of hair for quantitative analysis.[14]

Given that IR-MALDESI sensitivity toward EFV in hair was lower than other relevant ARVs calibrated in this work and that the method was capable of evaluating the longitudinal distribution of EFV at concentrations typically observed for ARVs in hair,[14–16,61,62] we anticipate that this approach has broad applicability for monitoring the disposition of ARVs in hair samples collected from patients. While MSI sample preparation has been minimized to reduce processing time and avoid axial and transverse analyte delocalization[25] and compromise the temporal record of drug use, solvent extraction[25] and longitudinal sectioning[27] steps will likely be explored in future analysis to improve limits of quantitation when targeting lower accumulating compounds. Since all patients examined were on the same fixed dose regimen of EFV, differences in the response observed in hair between patients may arise from metabolism or physiological incorporation into the hair strands. While explicating the contributing sources of these differences was beyond the scope of the current work, an approach to normalizing analyte response using a marker for melanin content is discussed in the next section.

Evaluating Hair Melanin Content by MSI

Drug response in hair can vary greatly depending on hair pigmentation, treatment, and texture. Cosmetic and ultrastructural alterations to hair through treatments such as bleaching and dyeing have been shown to reduce the presence of drug in hair.[64,65] The amount of drug incorporated in hair can correlate strongly to melanin content based on drug basicity,[35,37] and is likely one of the factors contributing to differences in EFV response observed between patients in the previous section. While Poetzsch et al. have recently demonstrated that melanin does not influence the ionization process of UV MALDI,[25] development of an MSI method to evaluate hair melanin content is needed to facilitate comparison in drug accumulation between different subjects, a necessity for an assessment of adherence based strictly on dose–response. Eumelanin, the predominate polymeric form of melanin, is composed mainly of the monomer unit 5,6-dihydroxyindole-2-carboxylic acid (DHICA). A common strategy for quantification of eumelanin involves the chemical oxidation of DHICA to PTCA,[39–41] as shown in Figure 4A. On the basis of the method of Szekely-Klepser et al.,[40] hair strands of different colors from multiple donors were adhered to a glass slide and 15% H_2O_2 was uniformly sprayed onto the surface of the hair strands. Once wetted, samples were allowed to incubate overnight prior to analysis. Targeted negative ion mode MS^2I monitoring of characteristic PTCA transitions, verified by direct infusion of a PTCA reference standard, was conducted on both pigmented and unpigmented hair strands as an initial validation step. Ion maps of $[PTCA - H]^-$ and fragments associated with the loss of one (*m/z* 154.01330) and two (*m/z* 110.02320) carboxylic acid units are shown in Figure 4B. These ion maps indicate that PTCA and its characteristic fragments were positively identified in the four pigmented hair strands analyzed but do not show any presence of the ions from gray, unpigmented hair strands (denoted by white asterisks in the overlaid images of Figure 4B) and served to confirm the PTCA peak assignment. PTCA response from hair strands with a range of pigmentation (blonde, brown, black, dyed) was then evaluated in a

full MS polarity switching MSI mode. PTCA ion abundance was observed to increase with darkening hair color (Figure 4C), and there is some indication that delocalization of PTCA away from the hair strands can occur during H_2O_2 incubation. Average PTCA response across each color hair strand is summarized in Figure 4D, with a range of almost an order of magnitude differentiating highly pigmented black strands from blonde. Dyed brown, chemically altered hair showed very little PTCA ion abundance. Additional assay optimization is expected to reduce the intrastrand variability in response (% RSD = 39–75%).

On the basis of the method for determining hair PTCA response, we evaluated the applicability of a normalization scheme for EFV in hair based on melanin content to facilitate direct interpatient comparison of drug accumulation. Strands ($n = 4$) from each of the three patients on therapy were first analyzed by IR-MALDESI for response to EFV before the strands were sprayed, incubated, and reanalyzed for EFV and PTCA. Optical images of the brown hair strands in Figure 5A show the depletion of pigmentation after the exposure to H_2O_2. Also seen in Figure 5A are ion maps of EFV distribution in hair strands, which do not indicate a significant difference in EFV ion abundance measured before and after exposure to H_2O_2. While exposure to peroxide-based bleaching creams has recently been shown to rapidly degrade the detectability of cocaine in hair during MSI analysis,[26] our results suggest that analysis of PTCA may be possible while still preserving the integrity of a drug bound in hair. Ion abundances of both EFV and PTCA were averaged based on longitudinal distance from the proximal end across all strands from each patient. The ion map of EFV response and average profiles of EFV distribution from each patient are shown in the top panel of Figure 5B, again indicating a 4-fold difference in response between Patient 1 and Patient 3 that is in good agreement with the LC–MS/MS response (Figure S-3). PTCA response between the brown hair strands from the patients varied (Figure S-4) and normalizing the per-voxel ion abundance of EFV ($[EFV + H]^+$) by that of PTCA($[PTCA - H]^-$), shown in the middle panel of Figure 5B, causes all profiles of patient response to fixed dose therapy to overlap within a standard deviation of measurement. EFV ionizes well in both positive and negative ionization modes, allowing us to also investigate normalizing the ion abundance of EFV ($[EFV - H]^-$) by PTCA($[PTCA - H]^-$) since we have shown recently that the % RSD for a normalization scheme can be sensitive to the ionization mechanism of the two ions compared based on potential differences in ionization efficiency.[33] The bottom panel of Figure 5B shows profiles of $[EFV - H]^-/PTCA - H]^-$, yielding similar results to $[EFV + H]^+/PTCA - H]^-$. This is the first evidence for a normalization approach to MSI drug response in hair based on melanin content. Determining the applicability of the technique for establishing adherence based on threshold drug response will require a much greater sample size of patients in future work, but the approach may hold great promise.

Additionally, imaging dosed hair strands over the range m/z 150–600 in both +ESI and −ESI yielded over 1000 peaks uniquely associated with hair. As shown in Figure S-5, the mass excess plot of these peaks, representing the difference between the nominal and monoisotopic ion mass, indicate a high degree of overlap with the mass excess distribution for lipid classes, particularly fatty acyls.[66] There is potential for discovery within these data of biomarkers for hair pigmentation without the requirement for an oxidation sample step, in a similar manner to recent identification of biomarker candidates for aging by MSI.[30]

CONCLUSIONS

The application of IR-MALDESI to the analysis of ARVs in hair for the purpose of characterizing drug adherence has been successfully demonstrated. Infrared laser desorption of hair samples penetrates through the cuticle layer of hair strands, allowing imaging of analytes in hair without any sample extraction and very minimal sample preparation for rapid analysis. Linear response of IR-MALDESI MSI relative to LC–MS/MS methods was observed for a range of HIV ARV agents over a 3-log concentration range. The high spatial resolution of IR-MALDESI MSI allows profiling of drug response along individual hair strands, offering a retrospective picture of a patient's drug adherence over a long temporal window. An approach to normalizing MSI response to drugs based on native melanin content of hair has also been demonstrated, facilitating the development of broadly applicable adherence evaluation criteria based solely on drug response.

Supplementary Material

Refer to Web version on PubMed Central for supplementary material.

Acknowledgments

The authors gratefully acknowledge financial support received from National Institutes of Health (Grants U19AI096113, R01AI111891, R01GM087964, and P30 AI50410).

REFERENCES

1. Haubrich RH, Little SJ, Currier JS, Forthal DN, Kemper CA, Beall GN, Johnson D, Dube MP, Hwang JY, McCutchan JA. the California Collaborative Treatment Group. AIDS. 1999; 13:1099–1107. [PubMed: 10397541]
2. Nieuwkerk PT, Oort FJ. JAIDS J. Acquired Immune Defic. Syndr. 2005; 38:445–448. [PubMed: 15764962]
3. Gross R, Bilker WB, Friedman HM, Strom BL. AIDS. 2001; 15:2109–2117. [PubMed: 11684930]
4. Haberer JE, Baeten JM, Campbell J, Wangisi J, Katabira E, Ronald A, Tumwesigye E, Psaros C, Safren SA, Ware NC, Thomas KK, Donnell D, Krows M, Kidoguchi L, Celum C, Bangsberg DR. PLoS Med. 2013; 10:e1001511. [PubMed: 24058300]
5. van der Straten A, Stadler J, Montgomery E, Hartmann M, Magazi B, Mathebula F, Schwartz K, Laborde N, Soto-Torres L. PLoS One. 2014; 9:e89118. [PubMed: 24586534]
6. Van Damme L, Corneli A, Ahmed K, Agot K, Lombaard J, Kapiga S, Malahleha M, Owino F, Manongi R, Onyango J, Temu L, Monedi MC, Mak'Oketch P, Makanda M, Reblin I, Makatu SE, Saylor L, Kiernan H, Kirkendale S, Wong C, Grant R, Kashuba A, Nanda K, Mandala J, Fransen K, Deese J, Crucitti T, Mastro TD, Taylor D, Grp FE-PS. N. Engl. J. Med. 2012; 367:411–422. [PubMed: 22784040]
7. van der Straten A, Van Damme L, Haberer JE, Bangsberg DR. AIDS. 2012; 26:F13–F19. [PubMed: 22333749]
8. Baumgartner WA, Hill VA, Blahd WH. J. Forensic Sci. 1989; 34:1433–1453.
9. Pragst F, Balikova MA. Clin. Chim. Acta. 2006; 370:17–49. [PubMed: 16624267]
10. Uematsu T. Clin. Pharmacokinet. 1993; 25:83–87. [PubMed: 8403740]
11. Beumer JH, Bosman IJ, Maes R. Int. J. Clin. Pract. 2001; 55:353–357. [PubMed: 11501221]
12. Huang Y, Gandhi M, Greenblatt RM, Gee WN, Lin ET, Messenkoff N. Rapid Commun. Mass Spectrom. 2008; 22:3401–3409. [PubMed: 18837069]
13. Huang Y, Yang QY, Yoon K, Lei Y, Shi R, Gee W, Lin ET, Greenblatt RM, Gandhi M. Anal. Bioanal. Chem. 2011; 401:1923–1933. [PubMed: 21847531]

14. Liu AY, Yang QY, Huang Y, Bacchetti P, Anderson PL, Jin CS, Goggin K, Stojanovski K, Grant R, Buchbinder SP, Greenblatt RM, Gandhi M. PLoS One. 2014; 9:e83736. [PubMed: 24421901]
15. Hickey MD, Salmen CR, Tessler RA, Omollo D, Bacchetti P, Magerenge R, Mattah B, Salmen MR, Zoughbie D, Fiorella KJ, Geng E, Njoroge B, Jin CS, Huang Y, Bukusi EA, Cohen CR, Gandhi M. JAIDS J. Acquired Immune Defic. Syndr. 2014; 66:311–315. [PubMed: 24694932]
16. Gandhi M, Ameli N, Bacchetti P, Anastos K, Gange SJ, Minkoff H, Young M, Milam J, Cohen MH, Sharp GB, Huang Y, Greenblatt RM. Clin. Infect. Dis. 2011; 52:1267–1275. [PubMed: 21507924]
17. Kleeberger CA, Phair JP, Strathdee SA, Detels R, Kingsley L, Jacobson LP. JAIDS J. Acquired Immune Defic. Syndr. 2001; 26:82–92. [PubMed: 11176272]
18. Parienti JJ, Massari V, Descamps D, Vabret A, Bouvet E, Larouze B, Verdon R. Clin. Infect. Dis. 2004; 38:1311–1316. [PubMed: 15127346]
19. Prideaux B, Stoeckli M. J. Proteomics. 2012; 75:4999–5013. [PubMed: 22842290]
20. Murphy RC, Hankin JA, Barkley RM. J. Lipid Res. 2008; 50(Suppl):S317–S322. [PubMed: 19050313]
21. Gode D, Volmer DA. Analyst. 2013; 138:1289–1315. [PubMed: 23314100]
22. Burnum KE, Frappier SL, Caprioli RM. Annu. Rev. Anal. Chem. 2008; 1:689–705.
23. Greer T, Sturm R, Li LJ. J. Proteomics. 2011; 74:2617–2631. [PubMed: 21515430]
24. Schwamborn K. J. Proteomics. 2012; 75:4990–4998. [PubMed: 22749859]
25. Poetzsch M, Steuer AE, Roemmelt AT, Baumgartner MR, Kraemer T. Anal. Chem. 2014; 86:11758. [PubMed: 25289728]
26. Cuypers E, Flinders B, Bosman IJ, Lusthof KJ, Van Asten AC, Tytgat J, Heeren RMA. Forensic Sci. Int. 2014; 242:103–110. [PubMed: 25047217]
27. Nakanishi T, Nirasawa T, Takubo T. J. Anal. Toxicol. 2014; 38:349–353. [PubMed: 24802158]
28. Shen M, Xiang P, Shi Y, Pu H, Yan H, Shen BH. Anal. Bioanal. Chem. 2014; 406:4611–4616. [PubMed: 24906693]
29. Porta T, Grivet C, Kraemer T, Varesio E, Hopfgartner G. Anal. Chem. 2011; 83:4266–4272. [PubMed: 21510611]
30. Waki ML, Onoue K, Takahashi T, Goto K, Saito Y, Inami K, Makita I, Angata Y, Suzuki T, Yamashita M, Sato N, Nakamura S, Yuki D, Sugiura Y, Zaima N, Goto-Inoue N, Hayasaka T, Shimomura Y, Setou M. PLoS One. 2011; 6:e26721. [PubMed: 22039541]
31. Robichaud G, Barry JA, Garrard KP, Muddiman DC. J. Am. Soc. Mass Spectrom. 2013; 24:92–100. [PubMed: 23208743]
32. Barry JA, Robichaud G, Bokhart MT, Thompson C, Sykes C, Kashuba ADM, Muddiman DC. J. Am. Soc. Mass Spectrom. 2014; 25:2038–2047. [PubMed: 24744212]
33. Bokhart M, Rosen E, Thompson C, Sykes C, Kashuba AM, Muddiman D. Anal. Bioanal. Chem. 2015; 407:2073–2084. [PubMed: 25318460]
34. Thompson CG, Bokhart MT, Sykes C, Adamson L, Fedoriw Y, Luciw PA, Muddiman DC, Kashuba ADM, Rosen EP. Antimicrob. Agents Chemother. 2015; 59:2944–2948. [PubMed: 25733502]
35. Rollins DE, Wilkins DG, Krueger GG, Augsburger MP, Mizuno A, O'Neal C, Borges CR, Slawson MH. J. Anal. Toxicol. 2003; 27:545–551. [PubMed: 14670132]
36. Slawson MH, Wilkins DC, Rollins DE. J. Anal. Toxicol. 1998; 22:406–413. [PubMed: 9788513]
37. Kronstrand R, Forstberg-Peterson S, Kagedal B, Ahlner J, Larson G. Clin. Chem. 1999; 45:1485–1494. [PubMed: 10471651]
38. Henderson GL, Harkey MR, Zhou CH, Jones RT, Jacob P. J. Anal. Toxicol. 1998; 22:156–165. [PubMed: 9547413]
39. Ito S, Wakamatsu K. Pigm. Cell Res. 2003; 16:523–531.
40. Szekely-Klepser G, Wade K, Woolson D, Brown R, Fountain S, Kindt E. J. Chromatogr. B. Anal. Technol. Biomed. Life Sci. 2005; 826:31–40.
41. Panzella L, Manini P, Monfrecola G, d'Ischia M, Napolitano A. Pigm. Cell Res. 2007; 20:128–133.

42. Rosen EP, Bokhart MT, Nazari M, Muddiman DC. Anal. Chem. 2015; 87:10483–10490. [PubMed: 26414177]
43. Robichaud G, Barry JA, Muddiman DC. J. Am. Soc. Mass Spectrom. 2014; 25:319–328. [PubMed: 24385399]
44. Sampson JS, Hawkridge AM, Muddiman DC. J. Am. Soc. Mass Spectrom. 2006; 17:1712–1716. [PubMed: 16952462]
45. Rosen EP, Bokhart MT, Ghashghaei HT, Muddiman DC. J. Am. Soc. Mass Spectrom. 2015; 26:899–910. [PubMed: 25840812]
46. Cochran K, Barry J, Robichaud G, Muddiman D. Anal. Bioanal. Chem. 2015; 407:813–820. [PubMed: 25081013]
47. Nazari M, Muddiman DC. Analyst. 2016
48. Jurchen JC, Rubakhin SS, Sweedler JV. J. Am. Soc. Mass Spectrom. 2005; 16:1654–1659. [PubMed: 16095912]
49. Olsen JV, de Godoy LMF, Li GQ, Macek B, Mortensen P, Pesch R, Makarov A, Lange O, Horning S, Mann M. Mol. Cell. Proteomics. 2005; 4:2010–2021. [PubMed: 16249172]
50. Kessner D, Chambers M, Burke R, Agus D, Mallick P. Bioinformatics. 2008; 24:2534–2536. [PubMed: 18606607]
51. Race AM, Styles IB, Bunch J. J. Proteomics. 2012; 75:5111–5112. [PubMed: 22641155]
52. Robichaud G, Garrard K, Barry J, Muddiman D. J. Am. Soc. Mass Spectrom. 2013; 24:718–721. [PubMed: 23536269]
53. Robichaud G, Barry J, Muddiman D. J. Am. Soc. Mass Spectrom. 2014:1–10. [PubMed: 24249043]
54. Dreisewerd K. Chem. Rev. 2003; 103:395–426. [PubMed: 12580636]
55. ChemAxon. [accessed October 8, 2015] http://www.chemicalize.org.
56. Kashuba ADM, Dyer JR, Kramer LM, Raasch RH, Eron JJ, Cohen MS. Antimicrob. Agents Chemother. 1999; 43:1817–1826. [PubMed: 10428898]
57. ViiV Healthcare Group. 2015 Retrieved from http://www.medicines.org.au/files/viptivic.pdf.
58. Moss DM, Siccardi M, Murphy M, Piperakis MM, Khoo SH, Back DJ, Owen A. Antimicrob. Agents Chemother. 2012; 56:3020–3026. [PubMed: 22450971]
59. Abel S, Back DJ, Vourvahis M. Antiviral Therapy. 2009; 14:607–618. [PubMed: 19704163]
60. Shalaeva M, Kenseth J, Lombardo F, Bastin A. J. Pharm. Sci. 2008; 97:2581–2606. [PubMed: 18228610]
61. Koss CA, Natureeba P, Mwesigwa J, Cohan D, Nzarubara B, Bacchetti P, Horng H, Clark TD, Plenty A, Ruel TD, Achan J, Charlebois ED, Kamya MR, Havlir DV, Gandhi M. AIDS. 2015; 29:825–830. [PubMed: 25985404]
62. Gandhi M, Mwesigwa J, Aweeka F, Plenty A, Charlebois E, Ruel TD, Huang Y, Clark T, Ades V, Natureeba P, Luwedde FA, Achan J, Kamya MR, Havlir DV, Cohan D, Prevention M, Toror HIVD. JAIDS J. Acquired Immune Defic. Syndr. 2013; 63:578–584. [PubMed: 24135775]
63. Nirogi R, Bhyrapuneni G, Kandikere V, Mudigonda K, Komarneni P, Aleti R, Mukkanti K. Biomed. Chromatogr. 2009; 23:371–381. [PubMed: 18937306]
64. Potsch L, Skopp G, Becker J. Int. J. Legal Med. 1995; 107:301–305. [PubMed: 7577693]
65. Jurado C, Kintz P, Menendez M, Repetto M. International Journal of Legal Medicine. 1997; 110:159–163. [PubMed: 9228567]
66. Sud M, Fahy E, Cotter D, Brown A, Dennis EA, Glass CK, Merrill AH Jr, Murphy RC, Raetz CR, Russell DW, Subramaniam S. Nucleic Acids Res. 2007; 35:D527–D532. [PubMed: 17098933]

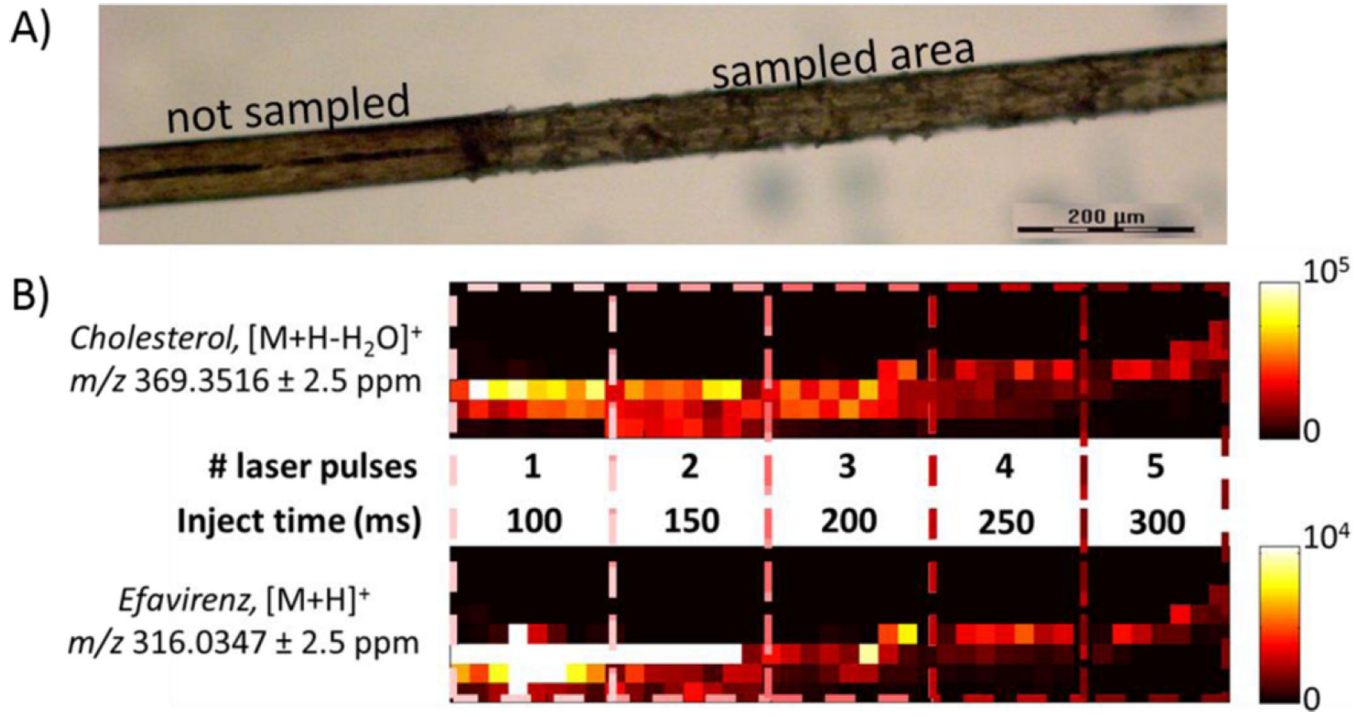

Figure 1.

Optimization of IR-MALDESI analysis of hair strands. (A) Optical image of hair strand indicating laser desorption of material in region analyzed by IR-MALDESI. (B) Ion maps of an endogenous lipid, cholesterol, and incubated ARV efavirenz collected with varying numbers of laser pulses (1–5) at each voxel.

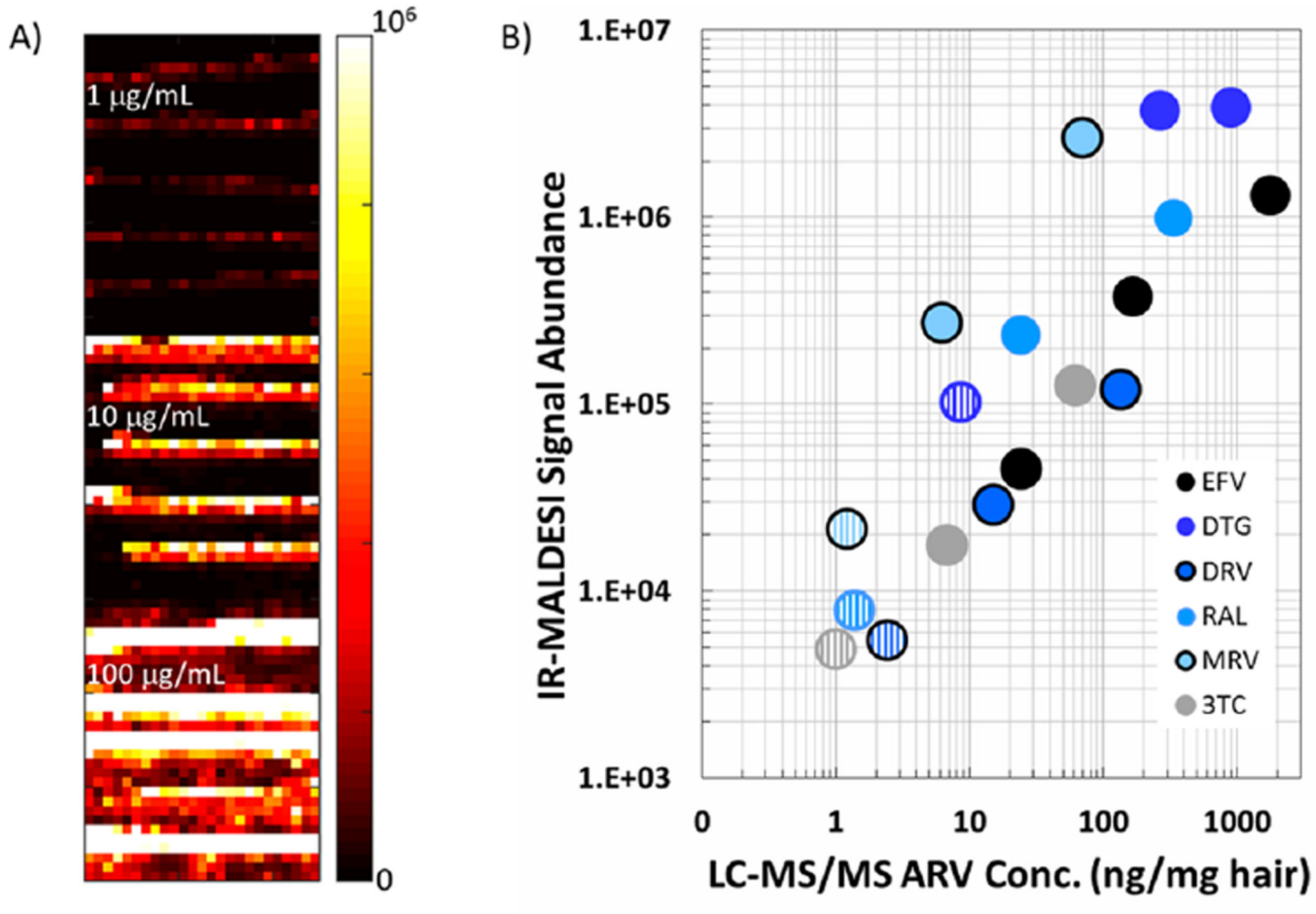

Figure 2.

Calibration of IR-MALDESI MSI response to ARV-incubated hair strands. (A) IR-MALDESI ion maps of EFV response, representative of other investigated ARVs, from strands incubated in stock solution concentrations of 1 µg/mL, 10 µg/mL, and 100 µg/mL as noted in each panel. (B) Log–log plot summarizing +ESI IRMALDESI response to all six ARVs relative to LC–MS/MS measurements of ARV accumulation from incubated hair strands. Linear plots comparing IR-MALDESI and LC–MS/MS results for each individual analyte are shown in the Supporting Information, Figure S-1.

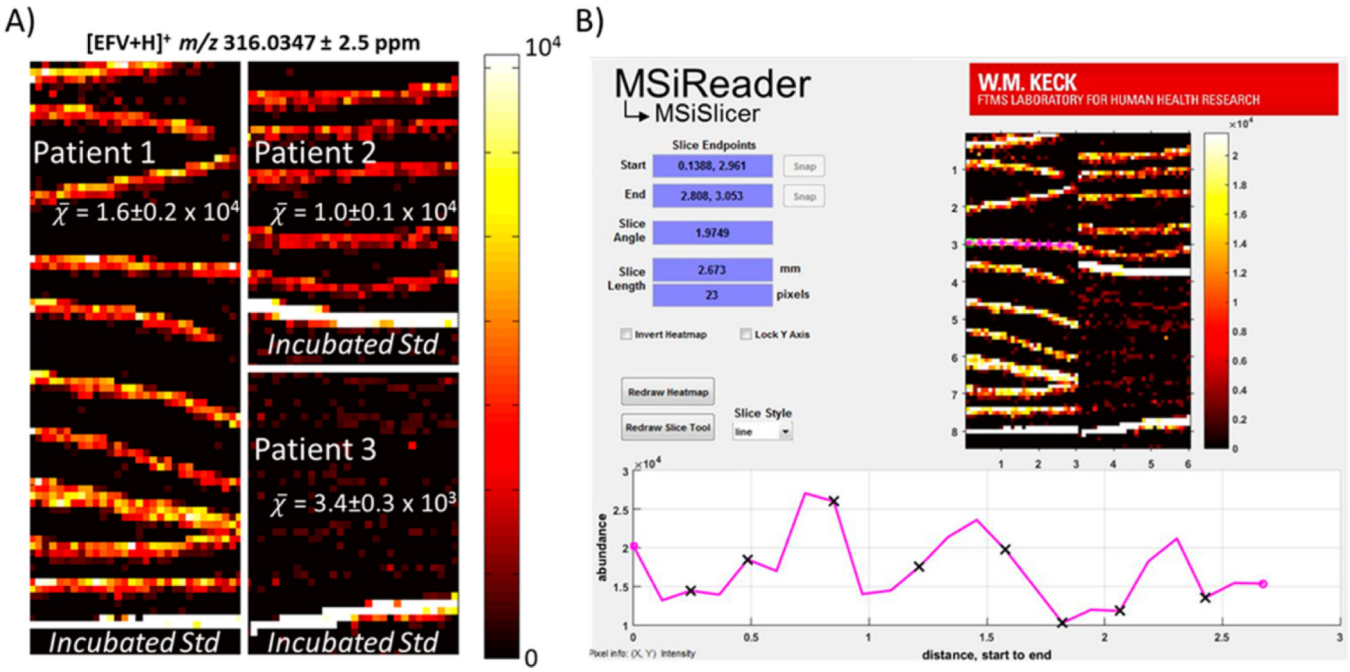

Figure 3.

Analysis of EFV in hair strands from three dosed patients. (A) IR-MALDESI MSI shows uniform longitudinal distribution of EFV in hair strands collected from virally suppressed dosed patients, with high intrapatient repeatability of response. (B) Longitudinal profiling of EFV response from proximal end of dosed hair strands using MSiReader.

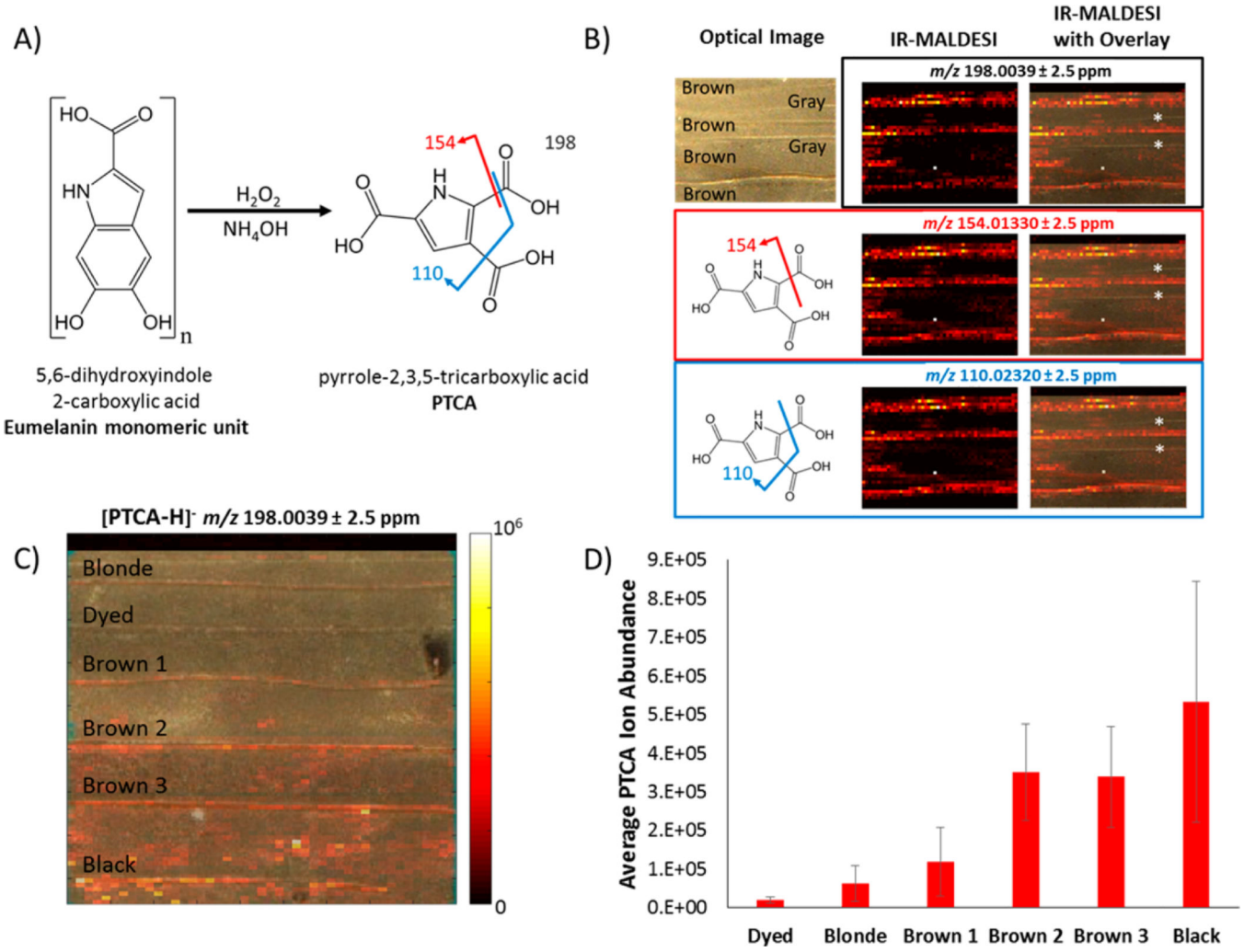

Figure 4.

(A) Scheme of melanin degradation to analytical target PTCA based on hair oxidation by 15% H_2O_2 and 1 M NH_4OH. (B) −ESI IR-MALDESI MS^2I ion maps of $[PTCA - H]^-$ (*m/z* 198.0039) and fragments associated with the loss of one (*m/z* 154.01330) and two (*m/z* 110.02320) carboxylic acid units from oxidized pigmented and unpigmented hair strands. Unpigmented, gray strands (denoted by white asterisks) show no response to PTCA. (C) Ion map of PTCA response from hair strands varying in color (dyed, blonde, brown, and black). D) Average $[PTCA - H]^-$ ion abundance from colored hair strands indicating increased abundance as hair color darkens.

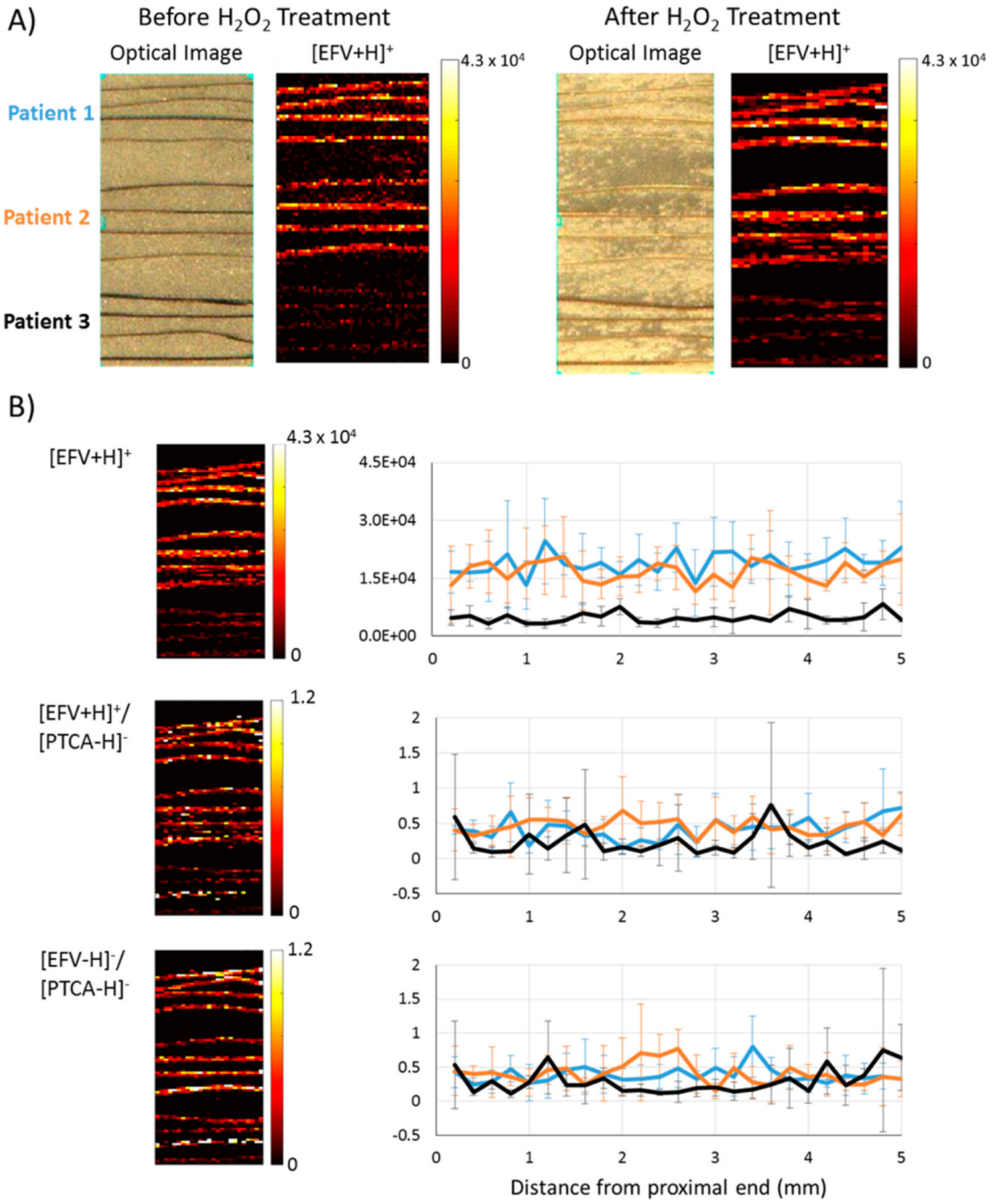

Figure 5.

(A) IR-MALDESI response to $[EFV + H]^+$ from strands ($n = 4$) of three dosed patients before (left) and after (right) oxidation of melanin by H_2O_2 indicating no significant degradation in response to EFV. (B) Top panel: ion map of $[EFV + H]^+$ (left) and average longitudinal profile (right) for each of three patients, indicating a 4-fold difference in response to accumulated EFV in hair. Middle panel: Normalization of $[EFV + H]^+$ response by $[PTCA - H]^-$ results in similar longitudinal profiles for each of three patients to fixed-

dose intake of EFV. Bottom panel: Comparative normalization approach for EFV, matching ionization mechanisms ($[EFV - H]^-/PTCA - H]^-$).